IARJSET
ISSN (Online) 2393-8021
ISSN (Print) 2394-1588
International Advanced Research Journal in Science, Engineering and Technology
ISO 3297:2007 Certified
Vol. 3, Issue 11, November 2016

A Novel Control Strategy for Design and Implementation of Neuro-Fuzzy Vector Control for Wind-Driven DFIG

Mr. G. Naidu[1], Mr. M. Sudheer Kumar[2]

PG Student, Department of EEE, ANITS, Visakhapatnam, India[1]

Assistant Professor, Department of EEE, ANITS, Visakhapatnam, India[2]

Abstract: This paper presents the neuro-fuzzy vector control for wind-driven DFIG to track the maximum wind power point. One configuration is realized by using back-to-back converters in rotor circuit and employing vector control. In this vector control the rotor side voltage source converter that allows independent control of the generated active and reactive as well as rotor speed to track the maximum wind power point. A neuro-fuzzy gain tuner is used to control the DFIG. Each neuro-fuzzy system has input as error value of generated speed active and reactive power. The choice of only one input to the system simplifies the design. Experimental investigations have also been conducted on a laboratory DFIG to verify the calculated results.

Keywords: Vector control, neuro-fuzzy, wind power generation .doubly-fed induction generator (DFIG).

I. INTRODUCTION

Due to its very good characteristics, DFIG is becoming the most popular for grid-connected wind power generation - where the terminal voltage and frequency are determined by the grid itself [1]-[8]. One configuration is realized by - using back-to-back converters in the rotor circuit and employing vector control. This allows the wind turbine to operate over a wide range of wind speed and maximize the annual energy production.

Fuzzy logic was used to control both active and reactive power generation in [1], [2] and [3], a fuzzy logic gain tuner was used to control the generator speed to maximize the total power generation as well as to control the reactive power generation through the control of rotor side currents as demonstrated in appendix A. The error signal of controlled variable was the single variable used as an input to the fuzzy system. In the above mentioned applications, the design of the fuzzy interference system was completely based on knowledge and experience of designer, and on the methods for tuning the membership functions so as to minimize the output error. To overcome the problems in design and tuning of fuzzy logic controller, a neuro fuzzy vector controller is proposed and it controls the DFIG speed, active and reactive powers independently .This neuro fuzzy vector controller utilizes 6 neuro-fuzzy gain tuners. Each of parameters, generator speed, active and reactive power, has 2 gain tuners. The input to each neuro fuzzy gain tuner is chosen to be error signal of controlled parameter. The choice of only one input to the system simplifies design.

In this paper dynamic model of wind driven DFIG is considered due to dynamic nature of the application. Since the machine performance depends on saturation conditions, both leakage flux and main flux saturations. In these controllers both proportional and integral gains are based up on error signals of generator speed, active and reactive power. The neuro-fuzzy systems are designed and trained to provide the best dynamic performance while tracking the maximum wind power point curve. Experimental investigations have also been conducted on a 2-KW laboratory

II. PROPORTIONAL AND INTEGRAL GAIN TUNERS

A. Conventional PI, Adaptive, and Fuzzy Gain Tuners

Conventional vector controllers [10] and [11] utilizes a PI controller with fixed Kp and Ki are determined by the zero/pole placement. If the system is highly nonlinear then we use adaptive controller .In this adaptive controller both Kp and Ki values depending up on the value of error [7]. The coefficients were selected such that, for the proportional gain, the system response is fast and with less over shoot and small settling time is obtained. While for the integral gain, it is reduce the over shoot and steady state error.

In [2], a fuzzy algorithm for tuning these two gains of PI controller is produced to have a good control performance when disturbances are present. The design of these rules is based on a qualitative knowledge, deduced from extensive simulation tests of conventional PI controller of the system for different values of K**p** and Ki for operating conditions.

B. Proposed Neuro-Fuzzy Gain Tuner

In neural networks learning methods are used to train and adjust the parameters of the membership functions as well as neuro-fuzzy system has learning methods.

IARJSET
ISSN (Online) 2393-8021
ISSN (Print) 2394-1588
International Advanced Research Journal in Science, Engineering and Technology
ISO 3297:2007 Certified
Vol. 3, Issue 11, November 2016

Neuro-adaptive learning techniques provide a method for Fuzzy modeling procedure to learn information about dataset. Then the parameters of membership functions that best allow associated fuzzy inference system to track given input/output data are computed as described in Appendix B.

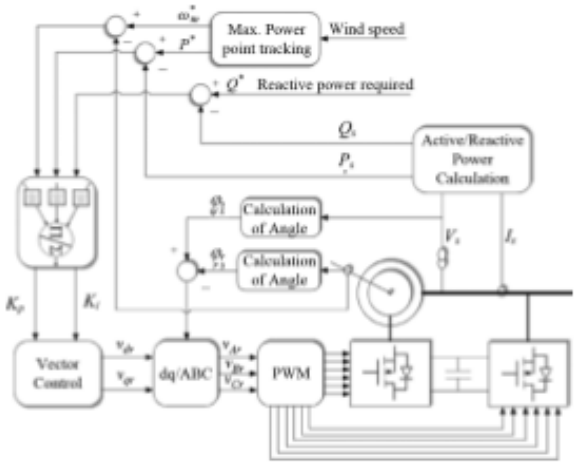

Fig. 1. Neuro-Fuzzy gain scheduler for vector control wind driven DFIG

In above Fig. 1 the vector control technique is presented, the wind speed is measured in order to determine the set of values for both the maximum output power of DFIG and the corresponding generator speed in order to track maximum power curve. The set of values are used to calculate error signal.

Error = Set value – measured value (wm, ps ,qs)

The absolute value of error signal is used to calculate the scheduled proportional and integral gains using neuro-fuzzy controller for each of speed, active and reactive power controllers. To apply the vector control to DFIG system, 6 neuro-fuzzy are trained in off line. 2 for each of speed, active and reactive power controllers. One unit is responsible for tuning the KP and other one for KI.

The developed neuro-fuzzy system is a first-order Sugeno type which has single input with ten Gaussian distribution member ship functions. It has ten if-then rules.

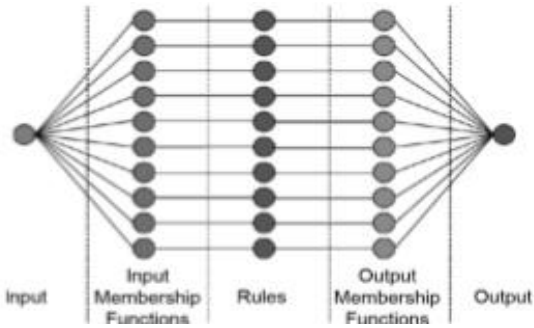

Fig 2. Simple structure of a single unit of the neuro-fuzzy gain scheduler

A simple structure of the developed neuro-fuzzy system is shown in Fig. 2 where the input is the error signal of the controlled variable of speed, active, or reactive power. The training is performed using the hybrid back-propagation algorithm. The training data used are collected from extensive simulations of the vector controller system with various PI gains so that the trained tuner can tune the PI gains online based on the knowledge of the different PI controllers under different operating conditions. The number of training epochs is set to 45 with an error tolerance of 10 .The number of epochs is chosen to be the highest number after which there is no significant reduction in the training error.

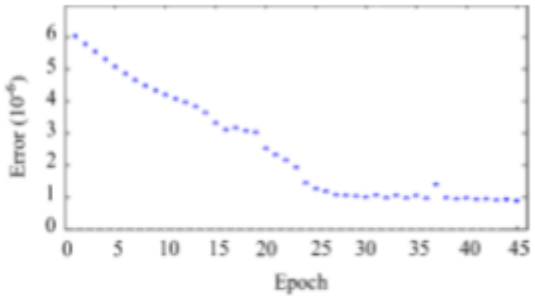

Fig. 3. Training error for the speed neuro-fuzzy gain tuner

Fig. 3 shows the error while training at each epoch for the neuro-fuzzy gain tuner of the speed controller.

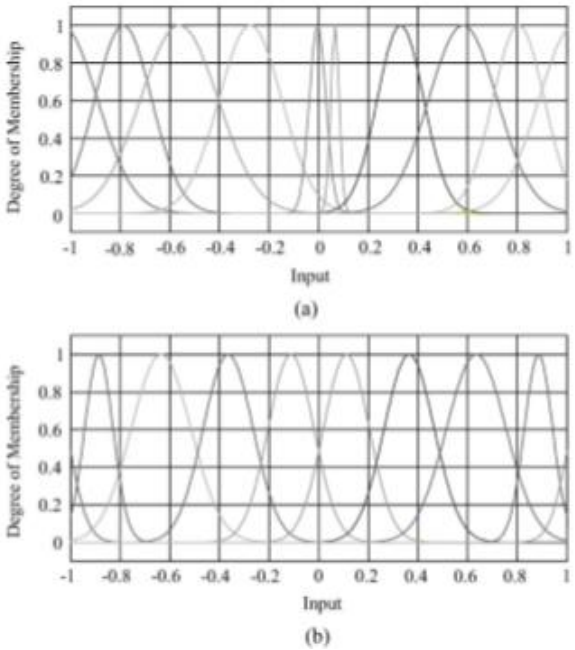

Fig.4. Input member ship functions for the proportional gain tuners. (a) Active power controller. (b) Speed controller.

After the training process the input membership functions for the neuro-fuzzy proportional gain tuner of both active power and speed are shown in Fig. 4. The output membership functions are chosen to be linear; the parameters of the ten linear output membership functions for the speed controller and active and reactive power controllers are listed in Tables I and II, respectively. The

IARJSET
ISSN (Online) 2393-8021
ISSN (Print) 2394-1588
International Advanced Research Journal in Science, Engineering and Technology
ISO 3297:2007 Certified
Vol. 3, Issue 11, November 2016

proportional and integral gains are in puts to the standard PI controller part of the vector controller to generate the control signals VDr and VQr .Then VDR and VQR along with the stator and rotor angles are used to generate signals for the back-to-back converter. The angle φs and φr are calculated as in Appendix A. These angles along with and help evaluate a three-phase stator voltage signal that is sent to a PWM controller to generate switching pulses for the back-to-back converters

TABLE I PARAMETERS OF THE LINEAR OUTPUT MEMBERSHIP FUNCTIONS OF THE SPEED CONTROLLER

	Proportional Gain		Integral Gain	
	p_i	r_i	p_i	r_i
MF 1	-387.0	-339.1	175.9	179.9
MF 2	-203.3	-117.4	52.38	46.06
MF 3	-171.7	-53.78	38.23	32.38
MF 4	-26.53	18.04	-1.405	19.37
MF 5	-197.6	3.579	26.85	23.29
MF 6	-63.12	26.77	-63.06	27.92
MF 7	-0.272	21.15	-7.523	19.54
MF 8	95.26	-14.91	-72.93	50.47
MF 9	146.9	-65.40	-79.23	70.89
MF 10	373.0	-323.0	-190.5	196.1

TABLE II PARAMETERS OF THE LINEAR OUTPUT MEMBERSHIP FUNCTIONS OF THE ACTIVE AND REACTIVE POWER CONTROLLERS

	Proportional Gain		Integral Gain	
	p_i	r_i	p_i	r_i
MF 1	-95.32	-56.11	140.6	142.8
MF 2	-15.95	13.24	16.96	26.35
MF 3	-4.948	22.90	5.534	17.16
MF 4	-2.390	11.85	6.732	29.42
MF 5	-2.023	11.63	3.208	28.50
MF 6	2.023	11.63	-3.208	28.50
MF 7	2.390	11.85	-6.732	29.42
MF 8	4.948	22.90	-5.534	17.16
MF 9	15.95	13.24	-16.96	26.35
MF 10	95.32	-56.11	-140.6	142.8

III. SIMULATION DIAGRAM AND RESULTS FOR SUBSYNCHRONOUS AND SUPER-SYNCHRONOUS OPERATIONS OF THE DFIG

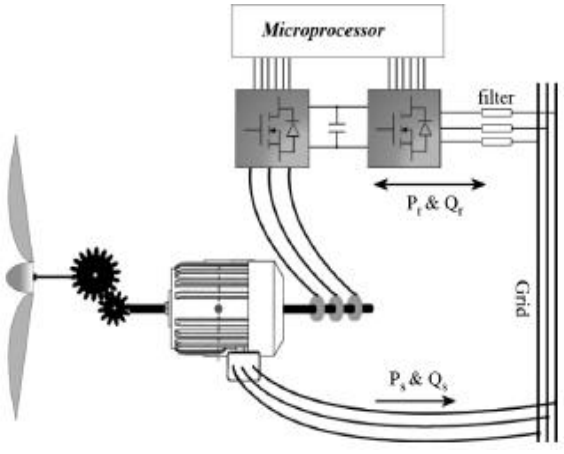

Fig. 5 system configuration. Wind-driven DFIG

In this paper we considered a grid connected wind driven DFIG as shown in above Fig. 5. While rotor side converter controls rotor speed and the active and reactive power output through d- and q- axis component of rotor voltage vqr and vdr, by neuro-fuzzy-based vector control strategy and grid side converter is controlled to maintain constant voltage level across capacitor. A filter is utilized to minimize the harmonics injected into grid due to the switching of power electronic devices.

A. DFIG used in the investigations

The 2-kW DFIG used for the investigations in this paper is driven by a laboratory dc motor, as shown in Fig. 6. The parameters of this machine are presented in Table III. The DFIG parameters have been determined by conducting dc, no-load, and locked-rotor tests on the machine

Fig 6. DFIG coupled to the dc motor in the experimental setup

TABLE III PARAMETERS OF THE DFIG USED IN THE INVESTIGATIONS

Rated power	2.0 kW	Magnetizing inductance	0.066 H
Rated stator voltage	120/208 V	Stator winding resistance	0.564 Ω
Rated rotor voltage	120/208 V	Rotor winding resistance	0.450 Ω
Rated frequency	60 Hz	Stator leakage inductance	0.0033 H
Rated Speed	1,720 rpm	Rotor leakage inductance	0.0032 H

These tests are explained in the IEEE standard of Test Procedure for Poly-Phase Induction Motors and Generators [12] and produce unsaturated machine parameters. In order to obtain a more realistic representation of the machine, saturation in the magnetic circuit along the main and leakage flux paths should be included in the machine model.

To determine the saturation characteristics of the magnetizing, stator and rotor leakage inductances, two unconventional tests are carried out. These test procedures are explained in detail in [13]. The no-load generator test at synchronous speed is carried out to determine the main flux saturation characteristics in Fig. 7(a).

IARJSET
ISSN (Online) 2393-8021
ISSN (Print) 2394-1588
International Advanced Research Journal in Science, Engineering and Technology
ISO 3297:2007 Certified
Vol. 3, Issue 11, November 2016

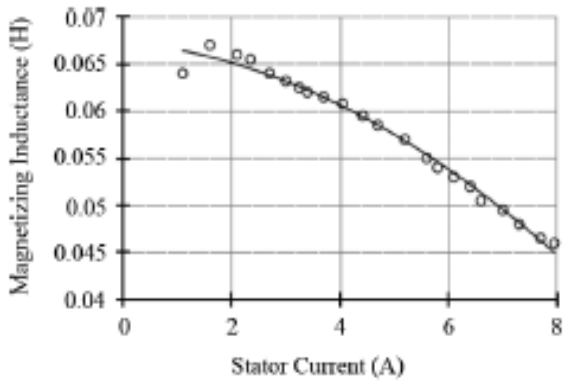

Fig. 7 (a) Magnetizing inductance

The terminal voltage–armature current curve with the machine unloaded and unexcited, and the open-circuit characteristics are determined twice; one on the stator and the other on the rotor, to determine the stator and rotor leakage inductance saturation characteristics in Fig. 7(b) and (c) c), respectively. This main flux path saturation has been represented in the generator model by modifying the unsaturated magnetizing inductance corresponding to the magnetizing current using Fig. 7(a). In order to take the leakage flux saturation into account, the unsaturated stator and rotor leakage inductances in the machine model have been modified employing the stator and rotor leakage inductance saturation characteristics in Fig. 7(b)and (c), respectively.

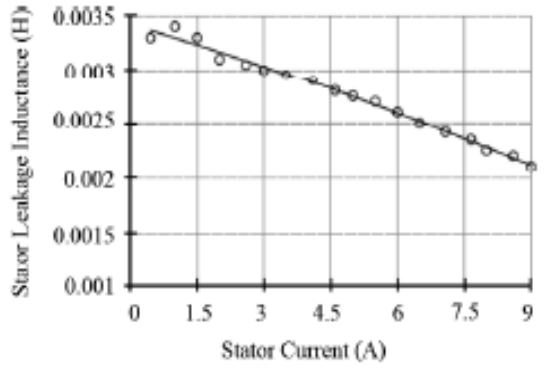

Fig. 7. (b) Stator leakage inductance

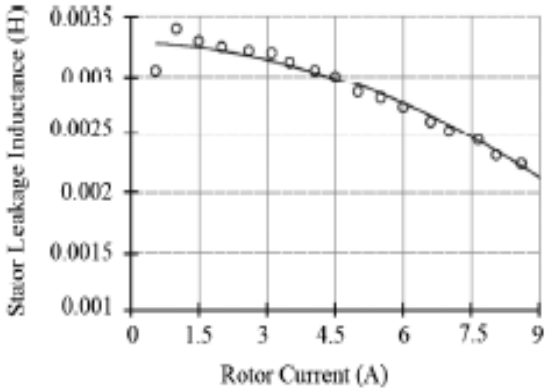

Fig. 7. (c) Rotor leakage inductance

B. Maximum Power Point Tracking

The output power changes as a function of the wind speed as well as the generator speed as shown in Fig. 8. To track the maximum power point, a lookup table is generated based on Fig. 8

For wind speeds less than 12 m/s and saved into the neuro-fuzzy vector controller. Wind speeds higher than 12 m/s are beyond the scope of this research.

When the measured wind speed changes, the lookup table will be searched to find the set values for both the maximum output power and the generator speed corresponding to the maximum power point. Although measuring the wind speed may have some drawbacks, it is the most accurate and easy way to change the generator speed in order to maximize the power generation. Major wind turbine manufacturers such as Vestas and Nordex have ultrasonic wind sensors in their V90-3.0 MW model [14] and N90/2500 kW model [15], respectively. The speed information from the sensor can be used for maximum power point tracking.

C. Sub- and Super-Synchronous Operations of the DFIG

The performance of the system employing the proposed neuro fuzzy gain tuner is examined under different operating conditions, as shown in Figs. 9 and 10.Two cases are considered in this paper. The first case investigates the sub synchronous operation where the wind speed changes from 7 to 8 m/s at t=1 s. According to Fig. 8, for the maximum power generation of 0.96 kWawindspeedof8m/s, the generatorsetspeedincreasesfrom1200t 1400rpm. The second case investigates the super-synchronous operation where the wind speed changes from9 to 11 m/s at t= 1 s. The generator set speed increases from 1600 to 1900 rpm according to the maximum power point curve in Fig. 8, where the corresponding power output is 1.86 kW at a wind speed of 11 m/s.

For both cases, the proposed neuro-fuzzy gain scheduler is employed The speed response, stator current, rotor line voltage, and rotor current for sub synchronous operation are shown in Fig. 9,while,for the super-synchronous operation, they are shown in Fig. 10

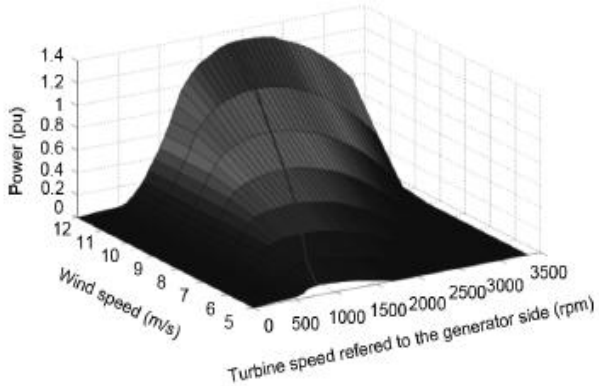

Fig. 8. Typical wind turbine power curves for different wind speeds showing maximum power point curve

IARJSET
ISSN (Online) 2393-8021
ISSN (Print) 2394-1588
International Advanced Research Journal in Science, Engineering and Technology
ISO 3297:2007 Certified
Vol. 3, Issue 11, November 2016

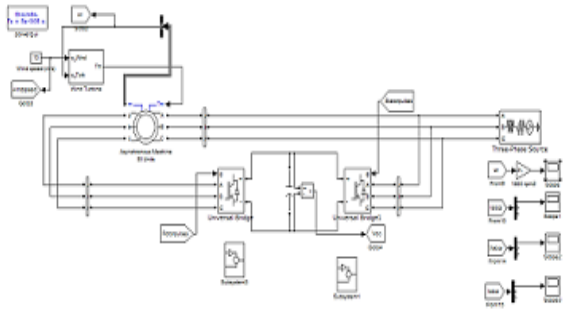

Simulation diagram

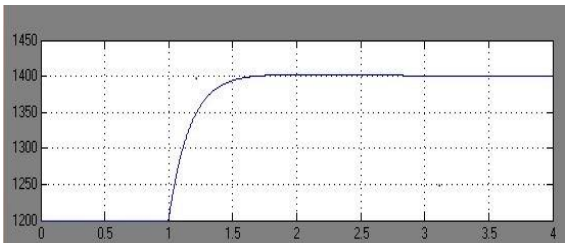

(a) Speed response
From above speed response DFIG speed at t=1s increased from 1200 rpm and reaches final value 1400 rpm

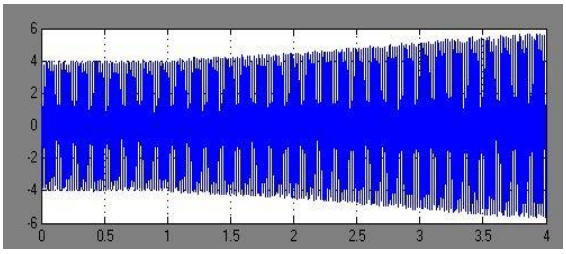

(b) Stator current
From above stator current response has current value 4A up to 1s and then increased

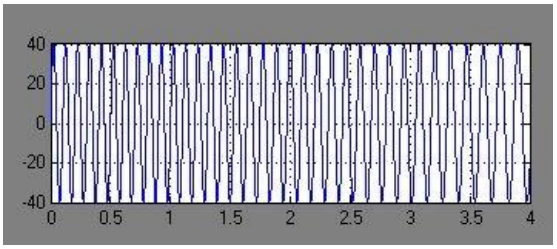

(c) Rotor line voltage.
From above Rotor line voltage response has voltage value 40V up to 1s and then increased

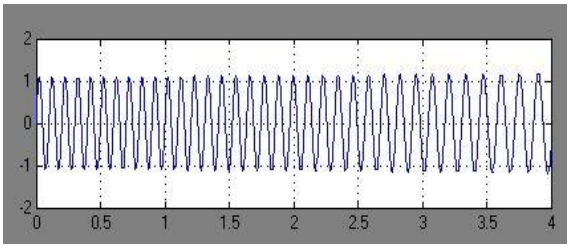

(d) Rotor current
From above rotor current response has current value 1A up to 1s and then increased

Fig.9. Calculated responses for sub synchronous operation (a) Speed response. (b) Stator current. (c) Rotor line voltage. (d) Rotor current

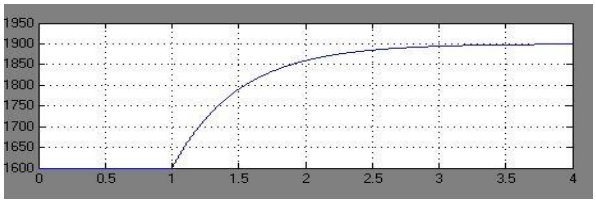

(a) Speed response
From above speed response DFIG speed at t=1s increased from 1600 rpm and reaches final value 1900 rpm

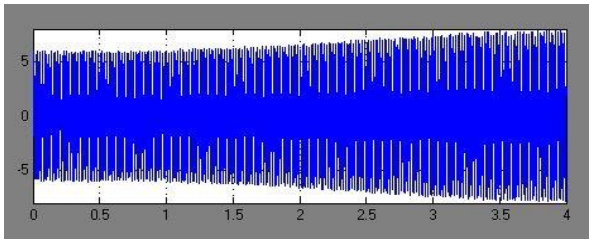

(b) Stator current
From above stator current response has current value 5A up to 1s and then increased as speed in super synchronous operation is greater than sub synchronous operation

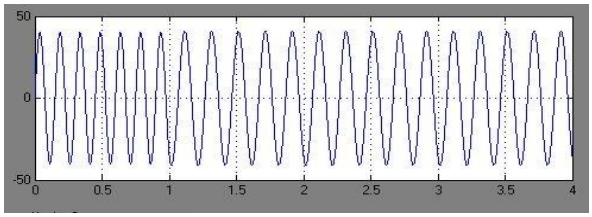

(c) Rotor line voltage
From above Rotor line voltage response voltage value 42V up to 1s and then increased as speed in super synchronous operation is greater than sub synchronous operation

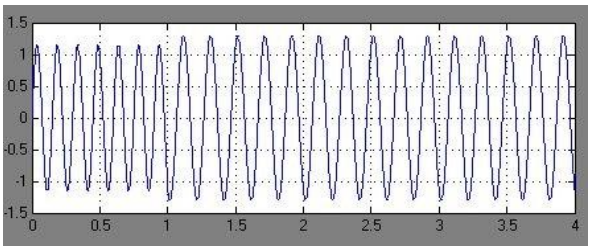

(d) Rotor current
From above rotor current response current value 1.1A up to 1s and then increased as speed in super synchronous operation is greater than sub synchronous operation

Fig. 10. Calculated responses for super-synchronous operation. (a) Speed response. (b) Stator current. (c) Rotor line voltage. (d) Rotor current

DOI 10.17148/IARJSET.2016.31139

IARJSET
ISSN (Online) 2393-8021
ISSN (Print) 2394-1588
International Advanced Research Journal in Science, Engineering and Technology
ISO 3297:2007 Certified
Vol. 3, Issue 11, November 2016

IV. EXPERIMENTAL DETERMINATION OF THE DFIG PERFORMANCE USING THE PROPOSED CONTROLLERS

The main objective is to validate the simulation results obtained in the previous section as well as investigate the performance of the DFIG when using different controllers. The types of controllers considered are: fuzzy logic [2],[3], and neuro-fuzzy. The performance of the DFIG system using the above mentioned controllers is compared to that of the conventional PI controller with constant gains.

While the system stability analysis employing these controllers is not the focus of this project, the controllers were developed with system stability in mind and it was observed that the system was stable during all experiments. As frequent and rapid changes of the controller gains may lead to instability, there is a limit as to how often and how fast the controller gains can be changed. The conventional PI controller has a proportional gain of 45 and an integral gain of 22.5. Numerous cases were considered and, for illustration purposes, two were chosen and will be demonstrated. For the ease of comparison, these two cases are chosen to be same as the two described in the simulation section. The first case investigates the sub synchronous operation of the DFIG with different controllers while the second case investigates the super-synchronous operation.

A.Sub synchronous Operation of the DFIG

In this case, the generator speed changes from 1200 to 1400 rpm. The resulting speed change for each controller is illustrated in Fig. 11(a).

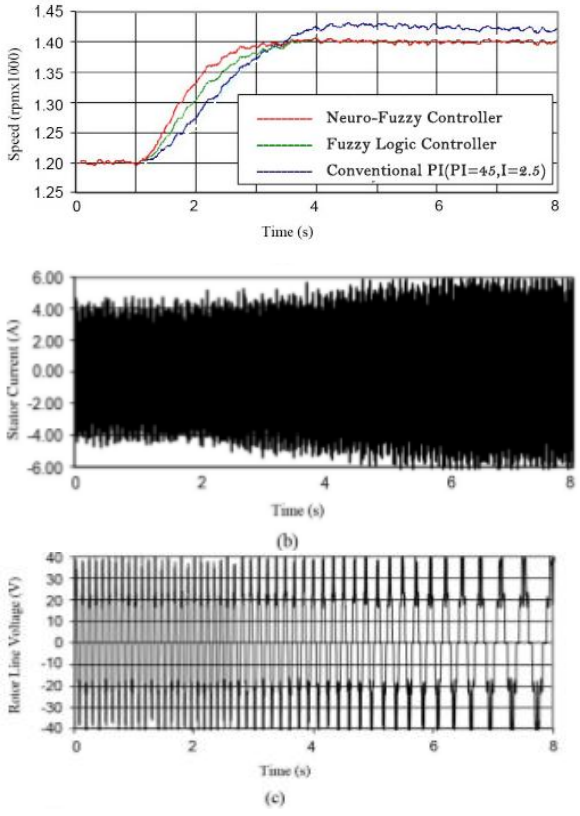

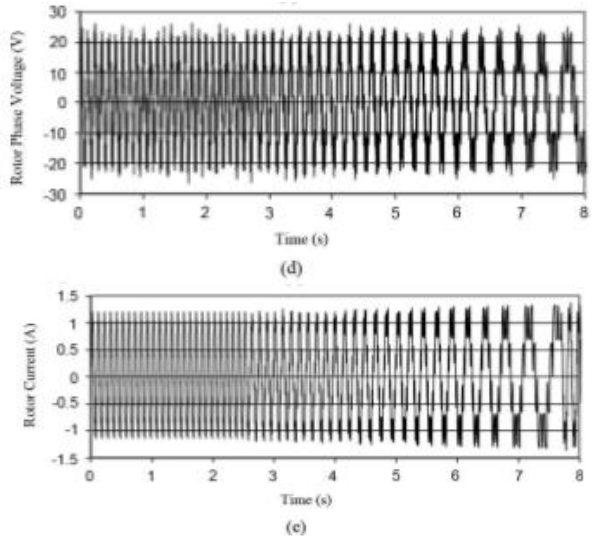

Fig. 11. Measured responses for sub synchronous operation. (a) Speed response. (b) Stator current. (c) Rotor line voltage. (d) Rotor phase voltage. (e) Rotor current

It can be seen from this figure and Table IV that the conventional PI controller with constant gain has a rise time of 2.8s with 2% overshoot and 1.5% steady-state error. On other hand other hand, the fuzzy PI gain scheduler has a rise time of 2 s and a settling time of 3 switch no over shoot and no steady-state error while the neuro-fuzzy PI gain scheduler has a rise time of 1.5 s and a settling time of 2.8 s with no overshoot and no steady-state error or the same case, the change in speed increased the stator active power production from 0.78 to 0.96 kW while the reactive power produced is kept constant at 0.80 kVAR.

TABLE IV CONTROLLERS'PERFORMANCE FOR SUBSYNCHRONOUS OPERATION

controller	Rise time (s)	Settling time (s)	Over shoot %	S.S. error %
Conv. PI	2.8	∞	2.0	1.5
fuzzy	2	3	0.0	0.0
Neuro-fuzzy	1.5	2.8	0.0	0.0

This rise in power production increased the stator current as shown in Fig. 11(b). At the rotor side, the increase in speed required an increase in the rotor current and rotor line voltage which are shown in Fig. 11(c)–(e), respectively. In order to increase the active power generation from 0.78 to 0.96 kW, an increase in the –axis component of the rot r current is required. However, there is no change in the -axis component of the rotor current since the reactive power generation has been kept constant. This increase in has resulted in an increase in the rotor current.

A. Super-Synchronous Operation of the DFIG

In the second case, the generator speed changes from 1600 to 1900 rpm. The resulting speed change for each controller is illustrated in Fig. 12(a). It can be seen from this figure and Table V that the conventional PI controller with

IARJSET
ISSN (Online) 2393-8021
ISSN (Print) 2394-1588
International Advanced Research Journal in Science, Engineering and Technology
ISO 3297:2007 Certified
Vol. 3, Issue 11, November 2016

constant gain has a rise time of 3.8 s and a settling time of 4.5 s with no overshoot and no steady-state error. On the other hand, the fuzzy PI gain scheduler has a rise time of 2.5 s and a settling time of 4.5 s with 0.6% overshoot and no steady-state error while the neuro-fuzzy PI gain scheduler has a rise time of 2.8 s and a settling time of 4.5 s with no overshoot and steady-state error. Although the fuzzy PI gain scheduler has a shorter rise time than that of the neuro-fuzzy PI gain scheduler in this case, it has the largest overshoot among the compared gain scheduler. For this case, the change in speed increased the stator active power production from 1.32 to 1.86 kW while the reactive power production is kept constant at 1 kVAR. This increase in power production increased the stator current as shown in Fig. 12(b). At the rotor side, the increase in speed required an increase in the rotor current and rotor line voltage which are shown in Fig. 12(c)–(e), respectively.

B. Comparison of the Results

It can be seen from Figs. 9 and 10 that the speed and stator and rotor quantities calculated by employing the neuro-fuzzy controller in Section IV-C are in good agreement with the experimentally measured ones shown in Figs. 11 to 12.

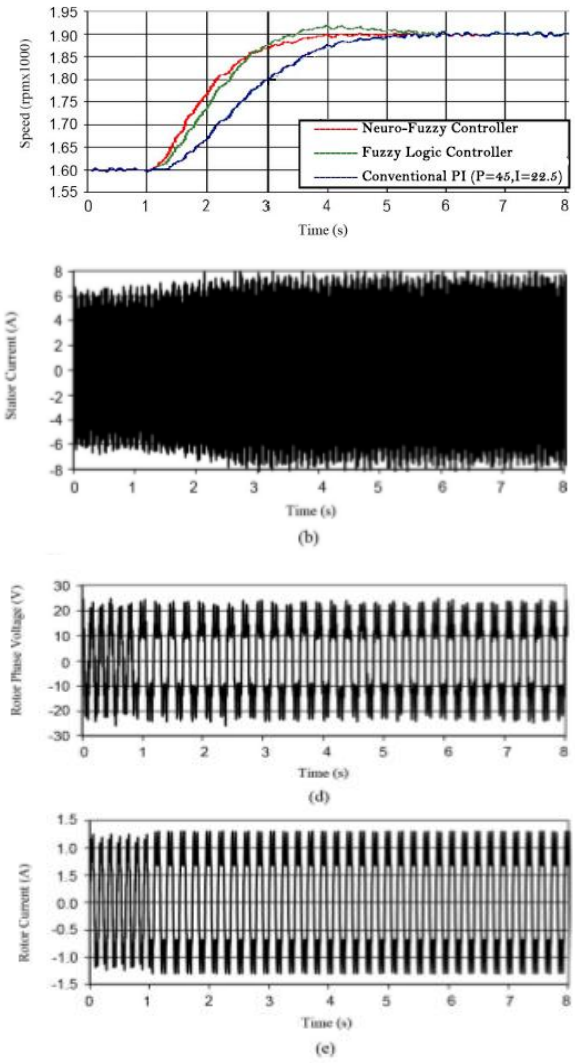

Fig.12. Measured responses for super-synchronous operation. (a) Speed response. (b) Stator current. (c) Rotor line voltage. (d) Rotor phase voltage. (e) Rotor current.

This indicates the accuracy of the proposed control system. The neuro-fuzzy PI gain scheduler enables proportional and integral gains within the vector control scheme to be changed depending on operating conditions. It can also be seen that using the proposed neuro-fuzzy controller, the dynamic response can be improved and more precise control is achieved in comparison to PI, and fuzzy logic controllers the proposed neuro-fuzzy PI gain scheduler achieved faster system response with almost no overshoot, shorter settling time and no steady-state error.

TABLE V CONTROLLERS'PERFORMANCE FOR SUPERSYNCHRONOUS OPERATION

controller	Rise time (s)	Settling time (s)	Over shoot %	S.S. error %
Conv. PI	3.8	4.5	0.0	0.0
fuzzy	2.5	4.5	0.6	0.0
Neuro-fuzzy	2.8	4.5	0.0	0.0

For DFIG operation in the entire speed range, it is well understood that the speed and frequencies of induction machines are such that the stator frequency is equal to the rotor electrical speed combined with the rotor frequency. It can be seen from Figs. 8 and 10 that the relation holds true for the super-synchronous mode of operation. Referring to Figs. 9(a) and (b) and 11(a) and (b), for sub synchronous mode, it is seen that the rotor speed settles to the new set point of 1400 rpm approximately at 4 s and the stator current has constant frequency of 60 Hz during the entire event; however, Figs. 11(c) and (d) and 9(c) and (d) show that the frequency of the rotor quantities decrease even after the speed has settled. Current research is underway to identify and resolve this apparent discrepancy

V. CONCLUSION

This paper presents a control method to maximize power generation of a wind-driven DFIG considering the effect of saturation in both main and leakage flux paths. This is achieved by applying vector control techniques with a neuro-fuzzy gain scheduler. The overall DFIG system performance using the proposed neuro-fuzzy gain tuner is compared to that using the conventional PI controllers. The generator speed response as well as the stator and rotor currents and the rotor voltages in response to a sudden change in the wind speed are presented .The main findings of the project can be summarized in the following points: 1) Traditional vector control schemes that employ a conventional PI controller with fixed proportional and integral gains give a predetermined response and cannot be changed. However, the proposed neuro-fuzzy PI gain scheduler enables proportional and integral gains within the vector control scheme to be changed depending on the operating conditions.2) It is demonstrated that, using the

IARJSET
ISSN (Online) 2393-8021
ISSN (Print) 2394-1588
International Advanced Research Journal in Science, Engineering and Technology
ISO 3297:2007 Certified
Vol. 3, Issue 11, November 2016

proposed controller, the system response can be improved and more precise control is achieved.3) The proposed neuro-fuzzy PI gain scheduler achieves faster system response with almost no overshoot, shorter settling time, and no steady-state error.

APPENDIX

A. Vector Control:

The vector control technique allows decoupled or independent control of both active and reactive power. This section reviews the basic vector control strategy in the case of DFIG. The stator flux oriented rotor current control, with decoupled control of active and reactive power, is adapted in this paper. The control schemes for the DFIG are expected to track a prescribed maximum power curve for maximum power capturing and to be able to control the reactive power generation the total active and reactive power generated can be obtained from the stator voltage and the d-and q-axis components of the stator current and can be expressed as

$$PS = 3/2\ vs\ iqs \quad QS = 3/2\ vs\ ids$$

The field oriented control is based on the dq-axis modeling, where the reference frame rotates synchronously with respect to the stator flux linkage. The direct axis of the reference frame overlaps the axis of stator flux making the axis component of stator flux φqs=0. In such a case, the following expression is

$$\varphi qs = Xs\ iqs + Xm\ iqr = 0$$

B. ANFIS Architecture: Currently, several neuro-fuzzy networks exist in the literature. Most notable is the adaptive network-based fuzzy inference system (ANFIS) developed by Jang [17]. Most neuro-fuzzy systems are developed based on the concept of neural methods on fuzzy systems. The idea is to learn the shape of membership functions for the fuzzy system efficiently by taking the advantage of adaptive property of the neural methods. Takagi, Sugeno, and Kang [18], [19] are known as the first to utilize this approach. Later, Jang [17] elaborated upon this idea and developed a systematic approach for the adaptation with illustrations of several successful applications. There are two types of fuzzy systems namely Mamdani and Sugeno. The Sugeno type has some advantages over the Mamdani type as it is computationally efficient and suitable for the application of optimization and adaptive techniques; works well with linear techniques (e.g., PID control), has guaranteed continuity of the output surface and is well suited to mathematical analysis. The fuzzy inference system used in this investigation is of Sugeno type.

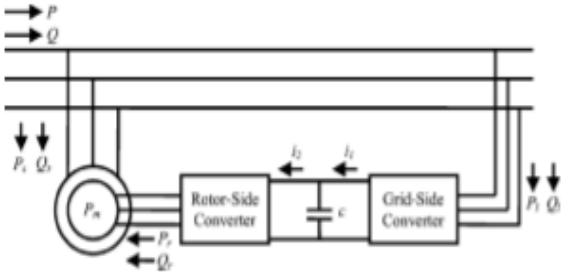

Fig. 13. Power-flow diagram in the case of a DFIG.

C. Control of Grid-Side Converter:

Through field oriented control of the rotor side converter, the maximum power speed profile can be tracked and the stator output reactive power can be separately controlled. The dc link capacitor provides a dc voltage to the rotor side converter and any attempt to store active power in the capacitor would raise its voltage level. Thus, to ensure stability of the system, power flow of the grid side converter, as indicated in Fig10

REFERENCES

[1] E. Kim, J. Kim, and G. Lee, "Power factor control of a doubly fed induction machine using fuzzy logic," in Proc. 5th Int. Conf. Electrical Machines and Systems, 2001, vol. 2, pp. 747–750.
[2] H. M. Jabr and N. C. Kar, "Fuzzy gain tuner for vector control of doubly-fed wind driven induction generator," in Proc. IEEE Canadian Conf. Elect. And Computer Engineering, 2006, pp. 2266–2269.
[3] H. M. Jabr and N. C. Kar, "Fuzzy logic based vector control of a doubly-fed induction generator in wind power application," J. Wind Eng., vol. 30, no. 3, pp. 201–224, May 2006.
[4] R. S. Peña, J. C. Clare, and G. M. Asher, "Doubly fed induction generator using back-to-back PWM converters and its application to variable speed wind-energy generation," IEE Proc. Electric Power Applications, vol. 143, no. 3, pp. 231–341, 1996.
[5] A. Tapia, G. Tapia, J. X. Ostolaza, and J. R. Sáenz, "Modeling and control of a wind turbine driven doubly fed induction generator," IEEE Trans. Energy Convers., vol. 18, no. 2, pp. 194–204, Jun. 2003.
[6] N. C. Kar and H. M. Jabr, "A novel PI gain scheduler for a vector controlled doubly-fed wind driven induction generator," in Proc. 8th IEEE Int. Conf. Electrical Machines and Systems, Sep. 2005, vol. 2, pp. 948–953.
[7] H. M. Jabr and N. C. Kar, "Adaptive vector control for slip energy re- covery in doubly-fed wind driven induction generator," in Proc. IEEE Canadian Conf. Electrical and Computer Engineering, May 2005, pp.759–762.
[8] Y. Tang and L. Xu, "A flexible active and reactive power control strategy for a variable speed constant frequency generating system," IEEE Trans. Power Electron., vol. 10, pp. 472–478, 1995.
[9] H. M. Jabr and N. C. Kar, "Leakage flux saturation effects on the transient performance of wound-rotor induction motor," J. Elect. Power Syst. Res., vol. 78, no. 7, pp. 1280–1289, 2008.
[10] R. Cárdenas and R. Peña, "Sensorless vector control of induction ma- chines for variable-speed wind energy applications," IEEE Trans. Energy Convers., vol. 19, pp. 196–205, 2004.
[11] G. Poddar, A. Joseph, and A. K. Unnikrishnan "Sensorless variable-speed controller for existing fixed speed wind power generator with unity-power-factor operation," IEEE Trans. Ind. Electron., vol. 50, no.5, pp. 1007–1015, Oct. 2003.
[12] IEEE Standard Test Procedure for Poly phase Induction Motors and Generators, IEEE Standard 1122004, 2004.
[13] R.N.Zavadil, Wind Generation Technical Characteristics for the NYSERDA Wind Impacts Study EnerNex Corporation, Tennessee , 2003.
[14] Vestas Wind Systems A/S:V90-3.0MW Wind Turbine BrochureApr.22 ,2009[Online].Available : http://www.vestas.com / vestas/ global/ En/ Products /Wind _ turbines /V90_3_0.htm
[15] NordexAG:N90/2500kWWindTurbineBrochureApr.22,2009 [Online]. Available: http://www.nordex-online.com/en/products-services/ wind-turbines/n90-25-mw.html
[16] P. Vas, Vector Control of AC Machines. New York: Oxford Univ. Press, 1990.
[17] J.S.Jang,"ANFIS:Adaptive-network-basedfuzzyinferencesystem," IEEE Trans.Syst., Man, Cybern., vol.23, no.3, pp. 665–684, May/ Jun. 1993.
[18] T.Takagi and M.Sugeno ,"Fuzzy identification of systems and its applications to modeling and control, "IEEE Trans.Syst. Man, Cybern, vol. 15, no. 1, pp. 116–132, Jan./Feb. 1985.